APL Electronic Devices ARTICLE pubs.aip.org/aip/aed

Consistent reporting of performances in Ga_2O_3 UV-C photodetectors

Cite as: APL Electron. Devices 1, 026108 (2025); doi: 10.1063/5.0255413
Submitted: 29 December 2024 • Accepted: 26 March 2025 •
Published Online: 10 April 2025

View Online Export Citation CrossMark

David Nicol,[1] Farnaz Hadizadeh,[1] Sean Douglas,[1] Steve Reynolds,[2] and Fabien C. P. Massabuau[1,a)]

AFFILIATIONS

[1] Department of Physics, SUPA, University of Strathclyde, Glasgow G4 0NG, United Kingdom
[2] School of Science and Engineering, University of Dundee, Dundee DD1 4HN, United Kingdom

[a)] Author to whom correspondence should be addressed: f.massabuau@strath.ac.uk

ABSTRACT

The study addresses the lack of consistency with reporting of Ga_2O_3 photodetector performances and assesses the impact of illumination intensity, illumination wavelength, and voltage bias on photodetector responsivity and time response. The approach reveals the electronic processes at play during Ga_2O_3 photodetector operation and provides qualitative insights into the defect spectroscopy of the materials. More importantly, the study highlights that high performance claims could be engineered through selective use of testing conditions and warns of malpractices when reporting performances, which could result in misleading comparisons. Finally, the study makes recommendations for future works reporting photodetector performances to enable normalization of performances, allowing fair comparisons across the literature. These recommendations are not specific to Ga_2O_3 and can be applied to other semiconductors.

I. INTRODUCTION

Ultraviolet-C (UV-C) sensing finds many applications in environmental monitoring, flame detection, missile warning systems, secure communications, astronomy, medical imaging, biochemical analysis, and ozone hole monitoring.[1] Gallium oxide (Ga_2O_3) is an emerging ultra-wide bandgap semiconductor and a leading candidate for next generation UV-C photodetectors.[2,3] This is a polymorphic compound, with known phases labeled α, β, κ, γ, and δ.[4,5] With a bandgap of ~5 eV, the material is naturally suited to detect UV-C radiations, and the prospects of alloying with other sesquioxides, e.g., Al_2O_3,[6] In_2O_3,[7] Fe_2O_3,[8] and Ti_2O_3,[9] offer much promise for performance tunability across the UV spectrum.

One of the key photodetector performances most commonly reported in the literature is the responsivity, which measures the photocurrent per unit of incident power, defined as

$$R = \frac{(I_{ph} - I_d)}{PA}, \tag{1}$$

where I_{ph} is the photocurrent, I_d is the dark current, P is the incident light intensity, and A is the effective illuminated area. Another important performance indicator commonly reported is the time response, which measures the time taken by the device to reach steady state operation as light is switched on (rise time τ_r) or switched off (decay time τ_d). These are conventionally measured as the time for the photocurrent to vary from 10% to 90% of its steady state value (and inversely for the decay time, from 90% to 10%).

However, the UV photodetector field does not adopt a standardized approach to record and report these performance indicators as in other fields, such as photovoltaics.[10–12] This lack of consistency results in a body of literature reporting performances obtained under very different experimental conditions, as illustrated in Table I in the context of UV-C photodetectors based on α-phase Ga_2O_3—a similar observations can be made for all the phases of Ga_2O_3.

In Ga_2O_3 resistive photodetectors, these performance indicators are strongly dependent on experimental conditions of illumination or bias. To illustrate this, Fig. 1 compares the photocurrent vs time plots of the same α-Ga_2O_3 photodetector illuminated using 250 nm light with 0.8 and 292 $\mu W/cm^2$ illuminating intensities and 10 V bias. We can clearly see that under the first conditions we obtain a device that compares in responsivity among the best of Table I, while the other set of conditions leads to time response on a par with the fast devices in Table I.

TABLE I. Comparison of performances for α-Ga_2O_3-based photodetectors. To illustrate the variations in experimental parameters, the list was restricted to metal–semiconductor–metal structures. In the electrode materials column, ohm. signifies reporting of linear I–V characteristics, and rect. signifies non-linear I–V characteristics. * Ouyang *et al.* investigated Si:Ga_2O_3 devices, with proportions of Si–Ga atoms in solution (from top to bottom): 0.3%, 1%, 2%, and 4%.

Reference	Illumination wavelength (nm)	Illumination intensity ($\mu W/cm^2$)	Bias (V)	Electrode materials	Electrode spacing (μm)	Electric field (10^3 V/cm)	Responsivity (A/W)	Rise time (s)	Decay time (s)	Year
Guo *et al.*[13]	254	130	5	Ti/Au (ohm.)	200	0.3	3.2×10^{-3}	~1	~1	2016
Lee *et al.*[14]	253	700	20	Pt (rect.)	30	6.7	0.76	···	···	2019
	266	- (Laser)	5			1.7	···	539×10^{-9}	89×10^{-6}	
Moloney *et al.*[15]	240	46	10	Ti/Au (ohm.)	100	1	1.17	>1	>1	2019
Qiao *et al.*[16]	244	···	5	Ni/Au (rect.)	5	10	3.36	···	···	2019
Hou *et al.*[17]	254	520	12	Ti/Au (ohm.)	5	24	11.5	>1	42×10^{-3}	2019
Muazzam *et al.*[18]	229	- (Lamp)	20	Ni/Au (rect.)	6	33	0.97	···	···	2019
Bae *et al.*[19]	254	~60	5	Pt/Au (rect.)	~15	~3.3	4.2×10^4	>10	>10	2021
Lee *et al.*[20]	- (Xe flash lamp)	6000	30	Ti/Au (ohm.)	15	20	0.19	2.6×10^{-6}	204×10^{-6}	2021
Sun *et al.*[21]	240	- (Lamp)	10	Ni/Au (rect.)	5	20	132.6	···	···	2021
	213	- (Laser)					···	2.3×10^{-6}	97×10^{-6}	
Kim *et al.*[22]	235	- (Lamp)	20	Ti/Au (ohm.)	8	25	550	5.47	0.44	2023
Almaev *et al.*[23]	235	27.2	10	Ti/Ni (rect.)	30	3.3	7.19×10^4	1190	72	2023
Ge *et al.*[24]	254	140	5	Ti/Au (ohm.)	···	···	~900	1.52	0.62	2023
Ouyang *et al.*[25]*	254	20	20	Ti/Au (ohm.)	20	10	0.22	6.63	0.63	2024
							4.62	4.45	0.62	
							45.47	2.31	0.57	
							323	1.02	0.55	
Li *et al.*[26]	254	31.2	3	Ti/Au (rect.)	~4	~7.5	3.76	3.89	2.85	2025

While the technology will ultimately dictate the performance requirements for the devices it will employ, this dependence of performance indicators on operating conditions makes comparisons across literature very challenging, if not misleading. This is even more significant if these comparisons are taken out of the context of purely device comparisons and used to conclude about the material quality. When the material is at such an early stage of development, it is important to enable rigorous comparisons to inform effective material improvement strategies. In this paper, we establish the effects of illumination intensity, illumination wavelength, and voltage bias on the responsivity and time response of Ga_2O_3 UV photodetectors in order to reveal the electronic processes at play in the material, but also warn of the influence of these parameters when comparing device performances. Finally, we propose good practices for future reporting of UV photodetector performances.

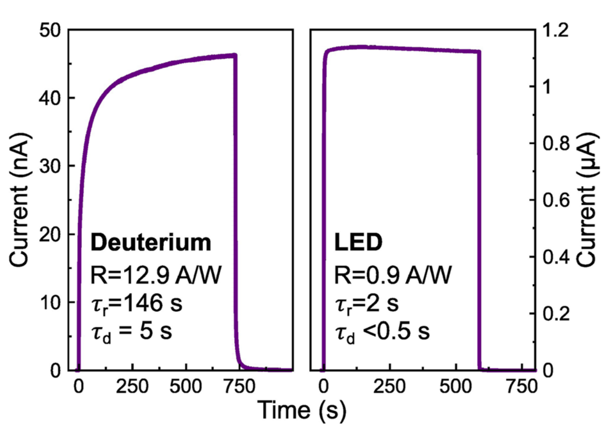

FIG. 1. Comparison of current-time plots of the same device illuminated by 250 nm light from a deuterium lamp (0.8 $\mu W/cm^2$) vs LED (292 $\mu W/cm^2$) and 10 V bias. The rise and decay times are based on 10%–90% figures as described in the text.

II. METHODS

An unintentionally doped 130 nm thick α-Ga_2O_3 film was grown on *c*-plane Al_2O_3 by plasma enhanced atomic layer deposition at 250 °C. Under these conditions, it is known that the resulting α-Ga_2O_3 film is grown epitaxially on the Al_2O_3 substrate with $[0001]_{Ga_2O_3} \| [0001]_{Al_2O_3}$ and $[11\bar{2}0]_{Ga_2O_3} \| [11\bar{2}0]_{Al_2O_3}$. The film consists dominantly of α-Ga_2O_3 columns, with amorphous and κ-Ga_2O_3 inclusions located between the columns,[27] and contains a $\sim 5 \times 10^{10}$ cm^{-2} density of threading dislocations.[28] The film exhibits an optical bandgap of 5.1 eV[29] and a broad luminescence spanning ~1.5–3.8 eV, peaking at ~2.5 eV, indicating a dominant contribution from donor–acceptor pair recombinations.[30] Following growth, the sample was annealed at 400 °C for 1 h in argon ambient and 1000 mbar pressure. The film was then processed into photodetector structures by depositing interdigitated Ti(20 nm)/Au(80 nm) metal electrodes to produce ohmic contacts.[15,31] The effective area of the photodetector is 0.425 mm^2, and interdigitated electrode spacing is ~100 μm.

Photoelectrical measurements were obtained using a Signatone probe station. The sample was biased, and photocurrent was measured using a Keithley 6487 picoammeter. Illumination was achieved using either a Thorlabs SLS204 deuterium lamp spectrally resolved by a Solar Laser Systems ML44 monochromator (spectral resolution 11 nm) or a Thorlabs LED250J 250 nm light emitting diode (LED), both fed into an optic fiber that illuminates a 1.13 mm^2 area of the sample with a ~45° incidence. A series of neutral density filters (Thorlabs NDUVxxB series) was used to attenuate the illumination power of the LED by up to five orders of magnitude. The illumination power was measured using a Thorlabs S130VC slim Si UV-extended photodiode with NIST-traceable calibration for the 200–1100 nm wavelength range and a 500 pW–0.5 mW power range.

III. RESULTS AND DISCUSSIONS

A. Effect of illumination intensity

Figure 2 investigates the effect of illumination intensity on the responsivity and time response of the photodetector. Here the illumination wavelength and bias were maintained at 250 nm and 10 V, respectively, while the illumination intensity was varied across five decades by means of neutral density filters. Looking at the log–log plot of the photocurrent vs intensity [Fig. 2(a) inset], we can identify two clear regimes of operations. A super-linear regime where $I_{ph} \propto P^{1.1}$ is observed for low illumination intensities, transitioning to a sub-linear regime where $I_{ph} \propto P^{0.7}$ for greater illumination intensities. Given the responsivity formula, these regimes translate into a slight increase of photodetector responsivity with illumination intensity, followed by a steep decrease for greater intensities—as can be seen in Fig. 2(a). The influence of illumination intensity is even more pronounced when looking at the time response, where the low intensity excitation yields devices that are too slow for many practical applications, while the high intensity region provides responses faster than the detection limit of our setup—limited by the circuit's RC constant and the ammeter's sampling frequency. In the context of comparing literature reports, this relationship highlights that employing different illumination intensity conditions can intrinsically induce up to an order of magnitude variation in responsivity and several orders of magnitude in time response. It is therefore not surprising that the fastest devices in Table I were reported with high illumination intensities (lasers and lamps at ~1000 μW/cm^2), while the best responsivities were obtained with illumination intensities of a few 10 s μW/cm^2.

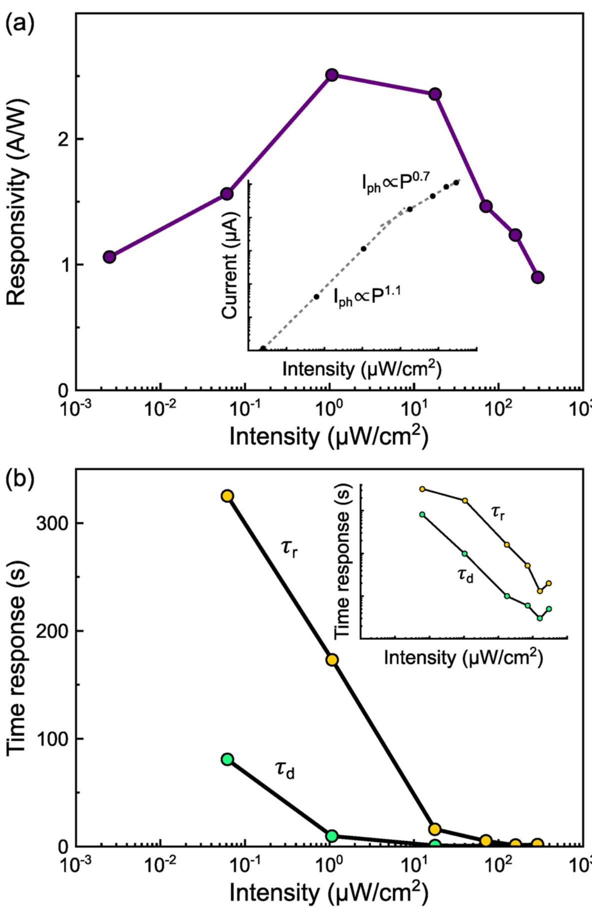

FIG. 2. Effect of illumination intensity on (a) responsivity and (b) time response. Data were taken under 250 nm illumination wavelength and 10 V bias. In the inset of (a), a log–log plot of photocurrent vs intensity is shown, highlighting a power-law relationship. In the inset of (b), a log–log plot of time response vs intensity is shown.

Analysis of the power law $I_{ph} \propto P^{\gamma}$ relationship can also be used to provide important insights into the electronic processes at play during photodetector operation.[32] To assist with the interpretation of the different power law regimes, we note that high gains attributed to hole trapping mechanisms have been reported in Ga_2O_3.[33,34] Under illumination, electrons are photoexcited to the conduction band, and holes become trapped. In the conduction band, the electrons can make many transits in the device before eventually recombining with the trapped holes, leading to the observed high gain.

A scenario where $\gamma = 1$ suggests a regime where the photocurrent varies linearly with illumination intensity, which also means that the responsivity should be constant irrespective of the illumination intensity. Fundamentally, this means that the free electron lifetime is independent of the illumination intensity.

A scenario where $\gamma > 1$ implies a super-linear behavior where relatively more carriers are released into the electrical circuit compared to the number of absorbed photons as intensity is increased. Super-linear behaviors have been reported in Ga_2O_3.[35] Under low excitation, i.e., at low carrier densities, an electron has a higher probability of interacting with an empty trap, thus reducing the effective time that the electron is in the conduction band. Rather than a single trapping event, multiple retrapping and strong interactions with the traps lead to a slow photocurrent rise time[36]—this process of long photocurrent rise time at low illumination intensity is well reflected in Fig. 2(b). Here, we have the case where the free carrier lifetime increases, causing the carrier density to increase at a faster rate than it can recombine, thus resulting in a super-linear behavior.

As the illumination intensity increases, we enter a sub-linear regime where $\gamma < 1$, meaning that the free carrier lifetime decreases with illumination intensity.[32] Sub-linear regimes have been observed in Ga_2O_3.[19,21,26,35] This effect could be attributed to the variation of quasi-Fermi level with illumination intensity. α-Ga_2O_3 has a large distribution of donor states within ~1 eV of the conduction band from a host of intrinsic defects and common impurities, including

H_i, H_O, V_O, and V_{Ga} complexes.[37–39] As the illumination intensity increases, the quasi-Fermi level shifts closer to the conduction band, thus populating the donor states during the transition. This in turn reduces the density of available traps, resulting in an increased likelihood of the electrons to remain in the conduction band and increasing the likelihood of recombination. Here, we see a process of the free carrier lifetime decreasing with increasing illumination intensity as a consequence of increased probability that the electrons are in the conduction band rather than in a trap, leading to a faster response time—as evident in Fig. 2(b). Bube proposed that the distribution of traps will have a significant effect on the value of γ.[32] Using a one-center recombination model, it was shown that γ could only be either 0.5 or 1, irrespective of the quasi-Fermi level position; however, if the density of traps varies with depth, a case arises where $0.5 \leq \gamma \leq 1$, which is what we and other groups have observed.[19,21,26,35] It seems that the density of defect states relative to the Fermi level defines these super- and sub-linear behaviors, but further study would be needed to understand the full range of factors affecting these power-law regions.

B. Effect of illumination wavelength

Figure 3 highlights the dependence of the performance indicators on illumination wavelength, obtained using the spectrally resolved deuterium lamp yielding a 0.4–1 μW/cm^2 intensity range. The responsivity plot has the typical shape expected for a photodetector and illustrates that the responsivity can change by orders of magnitude depending on the testing wavelength—Table I reports devices tested under 213 nm up to 266 nm illumination.

A high responsivity is obtained for illumination at and above the bandgap energy of the material, which for α-Ga_2O_3 is ~5.1–5.3 eV (i.e., 234–243 nm). This is due to the high absorption coefficient of the material at such wavelengths.[29] While the responsivity should, in theory, increase the shorter the wavelength, here we see that the responsivity plateaus and starts decreasing for wavelengths shorter than 210 nm. The shorter the wavelength, the greater the absorption coefficient, meaning that the photogenerated carriers are increasingly generated near the film surface. The decrease in responsivity for shorter wavelengths can therefore be indicative of either increased recombination (radiative or non-radiative) of photogenerated carriers at surface states or increased carrier density reducing lifetime. Looking at the time response, we observe that the device is faster for bandgap energy photons and slows down for shorter wavelength illumination, which supports an increasing role of surface defect states in the establishment of a photocurrent at these wavelengths.

The responsivity then rapidly decreases for wavelengths longer than the bandgap energy. The fact that carriers can be generated for sub-bandgap excitation hints at the presence of electronic states within the bandgap, which we know that Ga_2O_3 has plenty of.[29,37] The steepness of the decrease in responsivity is representative of the density of defect states,[40] which can thus be interpreted as an indicator of the quality of the material. We also observe that the time response of the device rapidly increases the longer the wavelength, reaching rise time values of hundreds of seconds for the longest wavelengths tested. Since long wavelength illumination causes a lower generation rate than near bandgap excitation, the effect of such illumination would effectively be somewhat similar to that of a low intensity illumination, hence causing a low responsivity and long time response similar to that seen in Fig. 2.

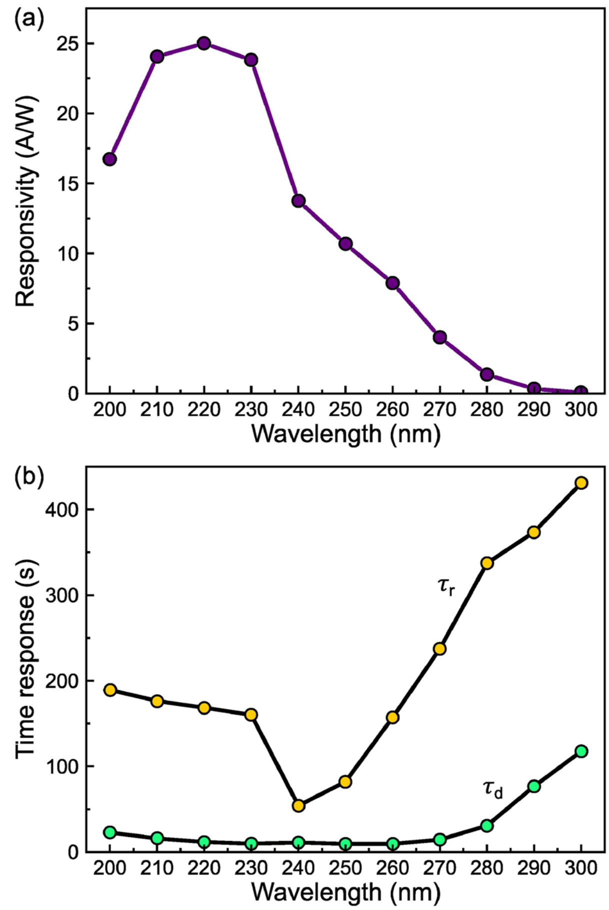

FIG. 3. Effect of illumination wavelength on (a) responsivity and (b) time response. Data were taken under the 0.4–1 μW/cm^2 illumination intensity range and 10 V bias.

C. Effect of voltage bias

The effect of voltage bias on responsivity and time response is shown in Fig. 4. The data were here obtained using the deuterium lamp spectrally resolved at 250 nm and an intensity of 0.8 μW/cm^2. We can see that the responsivity increases linearly with bias, which is expected due to the ohmic behavior of the Ti/Au contact on α-Ga_2O_3.[31] The applied bias is routinely mentioned in the literature, but a wide range of values can be used; e.g., Table I lists biases ranging from 5 to 30 V. However, since the effect of the bias is to generate an electric field that will move the carriers across the device, a more fundamental influence would be to consider the effect of the electric field on responsivity. This is even more significant as the bias is only meaningful in the context of a given device architecture through its electrode spacing. In our devices, the electrode spacing is ~100 μm, meaning the voltage sweep from 0 to 10 V corresponds to an electric field sweep from 0 to 10^3 V/cm. Looking at Table I from the electric field viewpoint, we observe that the electric field varies over two

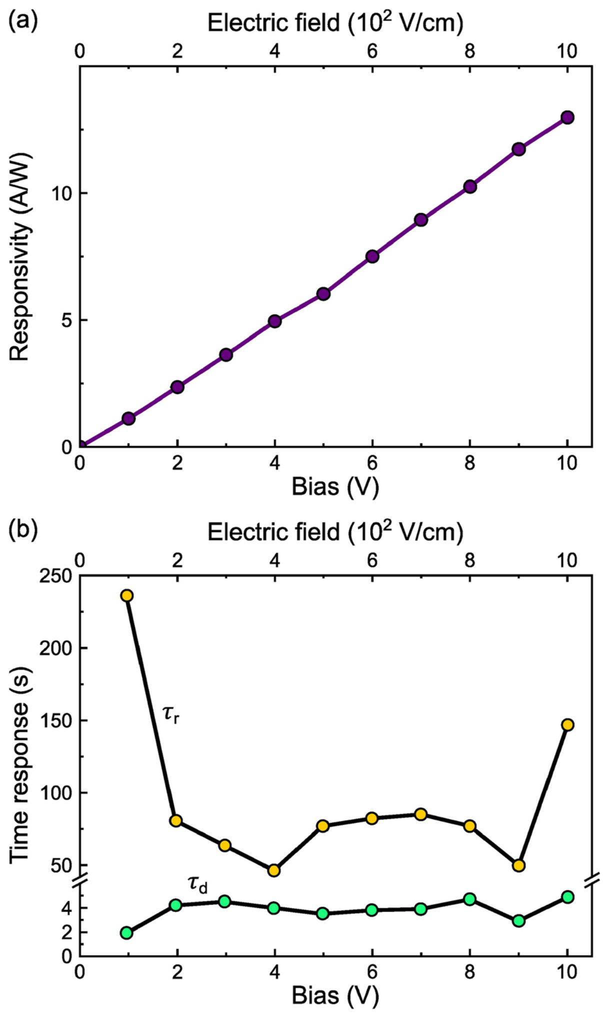

FIG. 4. Effect of bias (electric field) on (a) responsivity and (b) time response. Data were taken under 250 nm illumination wavelength and 0.8 μW/cm^2 intensity.

orders of magnitude (between 0.3×10^3 and 33×10^3 V/cm), and different metals are used to form ohmic or rectifying contacts, which puts some responsivity claims under new perspectives.

The effect of bias (or electric field) on the device time response [Fig. 4(b)] is unclear at this stage, where we see a slight, rather inconsistent decrease in rise time with electric field between 10^2 and 10^3 V/cm. Under these operational conditions, the longtime response is linked to multiple trapping events of the photogenerated electrons; however, it is unclear why such small variations of the electric field would affect the electron capture and release rates.

D. Good practices for performance reporting

In light of the testing conditions strongly impacting responsivity and time response, it is important to be transparent about all the experimental parameters used to characterize device performance to enable fair comparisons across the literature that would inform progress in material and device development. In particular, we recommend that future Ga_2O_3 photodetector studies implement the following points (as per the example in Table II):

- The illumination intensity must be clearly stated, and if possible, the power law $I \propto P^\gamma$ should be identified over several orders of magnitude range.
- The illumination wavelength must be clearly stated, and if possible, the wavelength dependence plot should be provided. If not possible, stating the rejection ratio as the ratio of responsivities between near-bandgap (UV-C) and sub-bandgap (e.g., visible, UV-A) illumination can be sufficient.
- The bias must be mentioned under the form of an electric field, and the ohmic/rectifying (polarity-dependent) behavior of the device must be identified.
- The 10%–90% time might not be the best-suited metric of time response for Ga_2O_3 photodetectors, as the 90% component dominates the measure and cannot be accurately determined since it falls on the slowly varying part of the stretched exponential transient.[41] Instead, we recommend using the 50% time (τ_{50}) as time response metrics.

At present, it is virtually impossible to rank the devices in Table I without making a series of assumptions. Only by following the above-mentioned advice can one "normalize" performance indicators for experimental conditions, enabling devices to be ranked based on their performance, facilitating progress in the field.

While the dependencies and subsequent reporting recommendations we highlight in this study are exemplified for Ga_2O_3 photodetectors, we want to point out that they can be generalized to photodetectors based on other semiconductors. The dependence of performance indicators on illumination wavelength and bias is naturally valid for other material systems, and the dependence on illumination intensity is also relevant as long as the $I_{ph} \propto P^\gamma$ power law yields $\gamma \neq 1$—which is routinely observed in a wide range of photodetector studies, including on III-N,[42–44] ZnO,[45–47] CdTe,[48–50] h-BN,[51] and WSe_2.[52]

Ultimately, the technology employing the photodetectors will dictate which operating conditions are relevant. When the technology readiness level of the field reaches that stage, devices should

TABLE II. Example of performance reporting for the photodetector investigated here, based on the conditions presented in Fig. 1 (left).

Sample	Illumination wavelength (nm)	Illumination intensity (μW/cm^2)	Electric field (10^3 V/cm)	Power law ($I \propto P^\gamma$)γ	Responsivity (A/W)	Rise time τ_{50r} (s)	Decay time τ_{50}(s)
This work	250	0.8	10 (ohmic)	1.1 ($P < 5$ μW/cm^2); 0.7 ($P > 5$ μW/cm^2)	12.9	7.9	0.9

be tested and reported using technology-specific standardized test conditions.

IV. CONCLUSIONS

We have investigated the effects of illumination intensity, illumination wavelength, and voltage bias on the performance of Ga_2O_3 UV-C photodetectors. The study shines light on the electronic processes at play in the semiconductor and helps obtain qualitative insights into the defect spectroscopy of the material. More importantly, we highlight the lack of consistency with reporting of Ga_2O_3 photodetector performance in the literature and that high performance claims could be engineered through selective use of testing conditions. We highlight malpractices when reporting Ga_2O_3 photodetector performance that could lead to misleading comparisons and make recommendations for future work reporting photodetector performances that would enable normalization of performances, allowing fair comparisons across the literature. While illustrated for Ga_2O_3 photodetectors, these recommendations can be applied to other semiconductors.

ACKNOWLEDGMENTS

The authors acknowledge support from the Royal Society (Grant No. RGS/R1/201236), the Engineering and Physical Sciences Research Council (Grant No. EP/T517938/1), and the UK Space Agency Enabling Technologies Programme (Grant No. UKSAG23_0043_ETP4-052).

AUTHOR DECLARATIONS

Conflict of Interest

The authors have no conflicts to disclose.

Author Contributions

David Nicol: Conceptualization (equal); Data curation (equal); Formal analysis (equal); Investigation (equal); Methodology (equal); Project administration (equal); Visualization (equal); Writing – original draft (equal); Writing – review & editing (equal). **Farnaz Hadizadeh**: Conceptualization (equal); Data curation (equal); Formal analysis (equal); Investigation (equal); Methodology (equal); Visualization (equal); Writing – original draft (equal); Writing – review & editing (equal). **Sean Douglas**: Conceptualization (supporting); Data curation (supporting); Formal analysis (supporting); Methodology (supporting); Project administration (supporting); Supervision (supporting); Visualization (supporting); Writing – original draft (equal); Writing – review & editing (equal). **Steve Reynolds**: Project administration (equal); Supervision (equal); Validation (equal); Visualization (equal); Writing – original draft (equal); Writing – review & editing (equal). **Fabien C. P. Massabuau**: Data curation (equal); Resources (equal); Supervision (equal); Validation (equal); Visualization (equal); Writing – original draft (equal); Writing – review & editing (equal).

DATA AVAILABILITY

The data that support the findings of this study are openly available in PurePortal at (https://doi.org/10.15129/9a9b96ef-15ef-4b9f-98ad-337ff27357ee), including raw data plots of time-dependent photocurrents and processed data used to plot the figures in the paper.

REFERENCES

[1] M. Kneissl, T.-Y. Seong, J. Han, and H. Amano, "The emergence and prospects of deep-ultraviolet light-emitting diode technologies," Nat. Photonics **13**, 233 (2019).

[2] J. Ding, P. Zhao, H. Chen, and H. Fu, "Ultraviolet photodetectors based on wide bandgap semiconductor: A review," Appl. Phys. A **130**, 350 (2024).

[3] C. Xie, X.-T. Lu, X.-W. Tong, Z.-X. Zhang, F.-X. Liang, L. Liang, L.-B. Luo, and Y.-C. Wu, "Recent progress in solar-blind deep-ultraviolet photodetectors based on inorganic ultrawide bandgap semiconductors," Adv. Funct. Mater. **29**, 1806006 (2019).

[4] R. Roy, V. G. Hill, and E. F. Osborn, "Polymorphism of Ga_2O_3 and the system Ga_2O_3–H_2O," J. Am. Chem. Soc. **74**, 719 (1952).

[5] I. Cora, F. Mezzadri, F. Boschi, M. Bosi, M. Čaplovičová, G. Calestani, I. Dódony, B. Pécz, and R. Fornari, "The real structure of ϵ-Ga_2O_3 and its relation to κ-phase," CrystEngComm **19**, 1509 (2017).

[6] R. Jinno, C. S. Chang, T. Onuma, Y. Cho, S.-T. Ho, D. Rowe, M. C. Cao, K. Lee, V. Protasenko, D. G. Schlom, D. A. Muller, H. G. Xing, and D. Jena, "Crystal orientation dictated epitaxy of ultrawide-bandgap 5.4- to 8.6-eV α-$(AlGa)_2O_3$ on m-plane sapphire," Sci. Adv. **7**, eabd5891 (2021).

[7] M. S. Williams, M. Alonso-Orts, M. Schowalter, A. Karg, S. Raghuvansy, J. P. McCandless, D. Jena, A. Rosenauer, M. Eickhoff, and P. Vogt, "Growth, catalysis, and faceting of α-Ga_2O_3 and α-$(In_xGa_{1-x})_2O_3$ on m-plane α-Al_2O_3 by molecular beam epitaxy," APL Mater. **12**, 011120 (2024).

[8] K. Kaneko, T. Nomura, and S. Fujita, "Corundum-structured α-phase Ga_2O_3–Cr_2O_3–Fe_2O_3 alloy system for novel functions," Phys. Status Solidi C **7**, 2467 (2010).

[9] A. Barthel, J. Roberts, M. Napari, M. Frentrup, T. Huq, A. Kovács, R. Oliver, P. Chalker, T. Sajavaara, and F. Massabuau, "Ti alloyed α–Ga_2O_3: Route towards wide band gap engineering," Micromachines **11**, 1128 (2020).

[10] IEC 61215-1-1:2021, Terrestrial photovoltaic (PV) modules - Design qualification and type approval - Part 1-1: Special requirements for testing of crystalline silicon photovoltaic (PV) modules, IEC, 2021.

[11] M. V. Khenkin, E. A. Katz, A. Abate, G. Bardizza, J. J. Berry, C. Brabec, F. Brunetti, V. Bulović, Q. Burlingame, A. Di Carlo, R. Cheacharoen, Y.-B. Cheng, A. Colsmann, S. Cros, K. Domanski, M. Dusza, C. J. Fell, S. R. Forrest, Y. Galagan, D. Di Girolamo, M. Grätzel, A. Hagfeldt, E. von Hauff, H. Hoppe, J. Kettle, H. Köbler, M. S. Leite, S. Liu, Y.-L. Loo, J. M. Luther, C.-Q. Ma, M. Madsen, M. Manceau, M. Matheron, M. McGehee, R. Meitzner, M. K. Nazeeruddin, A. F. Nogueira, Ç. Odabaşı, A. Osherov, N.-G. Park, M. O. Reese, F. De Rossi, M. Saliba, U. S. Schubert, H. J. Snaith, S. D. Stranks, W. Tress, P. A. Troshin, V. Turkovic, S. Veenstra, I. Visoly-Fisher, A. Walsh, T. Watson, H. Xie, R. Yıldırım, S. M. Zakeeruddin, K. Zhu, and M. Lira-Cantu, "Consensus statement for stability assessment and reporting for perovskite photovoltaics based on ISOS procedures," Nat. Energy **5**, 35 (2020).

[12] M. O. Reese, S. A. Gevorgyan, M. Jørgensen, E. Bundgaard, S. R. Kurtz, D. S. Ginley, D. C. Olson, M. T. Lloyd, P. Morvillo, E. A. Katz, A. Elschner, O. Haillant, T. R. Currier, V. Shrotriya, M. Hermenau, M. Riede, K. R Kirov, G. Trimmel, T. Rath, O. Inganäs, F. Zhang, M. Andersson, K. Tvingstedt, M. Lira-Cantu, D. Laird, C. McGuiness, S. J. Gowrisanker, M. Pannone, M. Xiao, J. Hauch, R. Steim, D. M. DeLongchamp, R. Rösch, H. Hoppe, N. Espinosa, A. Urbina, G. Yaman-Uzunoglu, J.-B. Bonekamp, A. J. J. M. van Breemen, C. Girotto, E. Voroshazi, and F. C. Krebs, "Consensus stability testing protocols for organic photovoltaic materials and devices," Sol. Energy Mater. Sol. Cells **95**, 1253 (2011).

[13] D. Y. Guo, X. L. Zhao, Y. S. Zhi, W. Cui, Y. Q. Huang, Y. H. An, P. G. Li, Z. P. Wu, and W. H. Tang, "Epitaxial growth and solar-blind photoelectric properties of corundum-structured α-Ga_2O_3 thin films," Mater. Lett. **164**, 364 (2016).

[14] S. H. Lee, K. M. Lee, Y.-B. Kim, Y.-J. Moon, S. Kim, D. Bae, S. B. Kim, Y. D. Kim, S. Kim, and S. W. Lee, "Sub-microsecond response time deep-ultraviolet photodetectors using α-Ga_2O_3 thin films grown via low-temperature atomic layer deposition," J. Alloys Compd. **780**, 400 (2019).

[15]J. Moloney, O. Tesh, M. Singh, J. W. Roberts, J. C. Jarman, L. C. Lee, T. N. Huq, J. Brister, S. Karboyan, M. Kuball, P. R. Chalker, R. A. Oliver, and F. C.-P. Massabuau, "Atomic layer deposited α-Ga_2O_3 solar-blind photodetectors," J. Phys. D: Appl. Phys. **52**, 475101 (2019).

[16]G. Qiao, Q. Cai, T. Ma, J. Wang, X. Chen, Y. Xu, Z. Shao, J. Ye, and D. Chen, "Nanoplasmonically enhanced high-performance metastable phase α-Ga_2O_3 solar-blind photodetectors," ACS Appl. Mater. Interfaces **11**, 40283 (2019).

[17]X. Hou, H. Sun, S. Long, G. S. Tompa, T. Salagaj, Y. Qin, Z. Zhang, P. Tan, S. Yu, and M. Liu, "Ultrahigh-performance solar-blind photodetector based on α-phase- dominated Ga_2O_3 film with record low dark current of 81 fA," IEEE Electron Device Lett. **40**, 1483 (2019).

[18]U. U. Muazzam, P. Chavan, S. Raghavan, R. Muralidharan, and D. N. Nath, "Optical properties of mist CVD grown α-Ga_2O_3," IEEE Photonics Technol. Lett. **32**, 422 (2020).

[19]J. Bae, D.-W. Jeon, J.-H. Park, and J. Kim, "High responsivity solar-blind metal-semiconductor-metal photodetector based on α-Ga_2O_3," J. Vac. Sci. Technol., A **39**, 033410 (2021).

[20]M. Lee, M. Yang, H.-Y. Lee, H. U. Lee, H. Lee, H. Son, and U. J. Kim, "The growth of HVPE α-Ga_2O_3 crystals and its solar-blind UV photodetector applications," Mater. Sci. Semicond. Process. **123**, 105565 (2021).

[21]X. Sun, Z. Wang, H. Gong, X. Chen, Y. Zhang, Z. Wang, X. Yu, F. Ren, H. Lu, S. Gu, Y. Zheng, R. Zhang, and J. Ye, "M-plane α-Ga_2O_3 solar-blind detector with record-high responsivity-bandwidth product and high-temperature operation capability," IEEE Electron Device Lett. **43**, 541 (2022).

[22]S. Kim, Y. Yoon, D. Seo, J.-H. Park, D.-W. Jeon, W. S. Hwang, and M. Shin, "Alpha-phase gallium oxide-based UVC photodetector with high sensitivity and visible blindness," APL Mater. **11**, 061107 (2023).

[23]A. Almaev, V. Nikolaev, V. Kopyev, S. Shapenkov, N. Yakovlev, B. Kushnarev, A. Pechnikov, J. Deng, T. Izaak, À. Chikiryaka, M. Scheglov, and A. Zarichny, "Solar-blind ultraviolet detectors based on high-quality HVPE α-Ga_2O_3 films with giant responsivity," IEEE Sens. J. **23**, 19245 (2023).

[24]K. Ge, D. Meng, X. Chen, X. Wang, X. Ji, and Z. Chen, "Solar-blind UV photoelectric properties of pure-phase α-Ga_2O_3 deposited on m-plane sapphire substrate," Appl. Phys. A **129**, 78 (2023).

[25]H. Ouyang, X. Wang, Y. Li, R. Wang, Y. Wang, N. Lin, T. He, H. Y. Feng, W. Mu, and Z. Jia, "High-performance solar-blind photodetector based on Si-doped α-Ga_2O_3 thin films grown by mist chemical vapor deposition," J. Alloys Compd. **1003**, 175593 (2024).

[26]G. Li, H. Peng, Y. Wang, S. Yao, M. Zhang, Y. Guo, and W. Tang, "α-Ga_2O_3 photodetector with responsivity over A/W level based on Sn-assisted mist-CVD," IEEE Sens. J. **25**, 2518 (2025).

[27]J. W. Roberts, J. C. Jarman, D. N. Johnstone, P. A. Midgley, P. R. Chalker, R. A. Oliver, and F. C.-P. Massabuau, "α-Ga_2O_3 grown by low temperature atomic layer deposition on sapphire," J. Cryst. Growth **487**, 23–27 (2018).

[28]R. Mullen, J. W. Roberts, P. R. Chalker, R. A. Oliver, B. Hourahine, and F. C. P. Massabuau, "Atomic scale observation of threading dislocations in α-Ga_2O_3," AIP Adv. **14**, 115018 (2024).

[29]D. Nicol, S. Reynolds, K. Barr, J. W. Roberts, J. J. Jarman, P. R. Chalker, and F. C.-P. Massabuau, "Constant photocurrent method to probe the sub-bandgap absorption in wide bandgap semiconductor films: The case of α-Ga_2O_3," Phys. Status Solidi B **261**, 2300470 (2024).

[30]D. Nicol, Y. Oshima, J. W. Roberts, L. Penman, D. Cameron, P. R. Chalker, R. W. Martin, and F. C.-P. Massabuau, "Hydrogen-related 3.8 eV UV luminescence in α-Ga_2O_3," Appl. Phys. Lett. **122**, 062102 (2023).

[31]F. Massabuau, D. Nicol, F. Adams, J. Jarman, J. Roberts, A. Kovács, P. Chalker, and R. Oliver, "Study of Ti contacts to corundum α-Ga_2O_3," J. Phys. D: Appl. Phys. **54**, 384001 (2021).

[32]R. Bube, *Photoelectronic Properties of Semiconductors* (Cambridge University Press, 1992).

[33]A. M. Armstrong, M. H. Crawford, A. Jayawardena, A. Ahyi, and S. Dhar, "Role of self-trapped holes in the photoconductive gain of β-gallium oxide Schottky diodes," J. Appl. Phys. **119**, 103102 (2016).

[34]A. Y. Polyakov, E. B. Yakimov, I. V. Shchemerov, A. A. Vasilev, A. I. Kochkova, V. I. Nikolaev, and S. J. Pearton, "Huge photosensitivity gain combined with long photocurrent decay times in various polymorphs of Ga_2O_3: Effects of carrier trapping with deep centers," J. Phys. D: Appl. Phys. **58**, 063002 (2025).

[35]S. Nakagomi, "Ultraviolet photodetector based on a beta-gallium oxide/nickel oxide/beta-gallium oxide heterojunction structure," Sensors **23**, 8332 (2023).

[36]Q. Zhao, W. Wang, F. Carrascoso-Plana, W. Jie, T. Wang, A. Castellanos-Gomez, and R. Frisenda, "The role of traps in the photocurrent generation mechanism in thin InSe photodetectors," Mater. Horiz. **7**, 252 (2020).

[37]A. Y. Polyakov, V. I. Nikolaev, E. B. Yakimov, F. Ren, S. J. Pearton, and J. Kim, "Deep level defect states in β-α-and ϵ-Ga_2O_3 crystals and films: Impact on device performance," J. Vac. Sci. Technol., A **40**, 020804 (2022).

[38]Z. Wang, X. Chen, F.-F. Ren, S. Gu, and J. Ye, "Deep-level defects in gallium oxide," J. Phys. D: Appl. Phys. **54**, 043002 (2021).

[39]H. Okumura and J. B. Varley, "MOCVD growth of Si-doped α-$(AlGa)_2O_3$ on m-plane α-Al_2O_3 substrates," Jpn. J. Appl. Phys. **63**, 075502 (2024).

[40]P. Mazzolini, J. B. Varley, A. Parisini, A. Sacchi, M. Pavesi, A. Bosio, M. Bosi, L. Seravalli, B. M. Janzen, M. N. Marggraf, N. Bernhardt, M. R. Wagner, A. Ardenghi, O. Bierwagen, A. Falkenstein, J. Kler, R. A. De Souza, M. Martin, F. Mezzadri, C. Borelli, and R. Fornari, "Engineering shallow and deep level defects in κ-Ga_2O_3 thin films: Comparing metal-organic vapour phase epitaxy to molecular beam epitaxy and the effect of annealing treatments," Mater. Today Phys. **45**, 101463 (2024).

[41]A. Y. Polyakov, A. V. Almaev, V. I. Nikolaev, A. I. Pechnikov, V. I. Shchemerov, A. A. Vasilev, E. B. Yakimov, A. I. Kochkova, V. V. Kopyev, B. O. Kushnarev, and S. J. Pearton, "Mechanism for long photocurrent time constants in α-Ga_2O_3 UV photodetectors," ECS J. Solid State Sci. Technol. **12**, 045002 (2023).

[42]C. Pernot, A. Hirano, M. Iwaya, T. Detchprohm, H. Amano, and I. Akasaki, "Low-intensity ultraviolet photodetectors based on AlGaN," Jpn. J. Appl. Phys. **38**, L487 (1999).

[43]H. Wang, M. Feng, Y. Zhong, X. Chen, H. Gao, E. Yilmaz, Q. Sun, and H. Yang, "Ultrahigh-responsivity ultraviolet photodetectors based on AlGaN/GaN double-channel high-electron-mobility transistors," ACS Photonics **11**, 180 (2024).

[44]Y. Du, S. Yin, Y. Li, J. Chen, D. Shi, E. Guo, H. Zhang, Z. Wang, Q. Qin, C. Zou, T. Zhai, and L. Li, "Liquid-metal-assisted synthesis of patterned GaN thin films for high-performance UV photodetectors array," Small Methods **8**, 2300175 (2024).

[45]H.-C. Wang, Y. Hong, Z. Chen, C. Lao, Y. Lu, Z. Yang, Y. Zhu, and X. Liu, "ZnO UV photodetectors modified by Ag nanoparticles using all-inkjet-printing," Nanoscale Res. Lett. **15**, 176 (2020).

[46]H. Lu, X. Zhou, T. Liang, L. Zhang, and S. Zhang, "Nonlinear photocurrent-intensity behavior of amorphous InZnO thin film transistors," Appl. Phys. Lett. **112**, 042103 (2018).

[47]S. Mondal, S. Ghosh, and D. Basak, "Extraordinarily high ultraviolet photodetection by defect tuned phosphorus doped ZnO thin film on flexible substrate," Mater. Res. Bull. **144**, 111490 (2021).

[48]B. Ren, J. Zhang, M. Liao, J. Huang, L. Sang, Y. Koide, and L. Wang, "High-performance visible to near-infrared photodetectors by using (Cd,Zn)Te single crystal," Opt. Express **27**, 8935 (2019).

[49]B. G. Valmik, M. P. Deshpande, S. V. Bhatt, V. Sathe, H. R. Bhoi, P. Rajput, and S. H. Chaki, "Investigation and fabrication of cadmium telluride (CdTe) single crystal as a photodetector," Physica B **614**, 413027 (2021).

[50]M. Shaygan, K. Davami, N. Kheirabi, C. K. Baek, G. Cuniberti, M. Meyyappan, and J.-S. Lee, "Single-crystalline CdTe nanowire field effect transistors as nanowire-based photodetector," Phys. Chem. Chem. Phys. **16**, 22687 (2014).

[51]M. Qiu, Z. Jia, M. Yang, K. Nishimura, C.-T. Lin, N. Jiang, and Q. Yuan, "High detectivity solar blind photodetector based on mechanical exfoliated hexagonal boron nitride films," Nanotechnology **34**, 285204 (2023).

[52]C. Zhou, S. Raju, B. Li, M. Chan, Y. Chai, and C. Y. Yang, "Self-driven metal–semiconductor–metal WSe_2 photodetector with asymmetric contact geometries," Adv. Funct. Mater. **28**, 1802954 (2018).